

# LOW COST 3D LOCALIZATION SYSTEM FOR APPLICATIONS ON AERIAL ROBOTS

**Antônio Padilha Lanari Bó, antonio.plb@gmail.com**

**Geovany Araújo Borges, gaborges@ene.unb.br**

Laboratório de Automação e Robótica - LARA

Grupo de Robótica, Automação e Visão - GRAV

Departamento de Engenharia Elétrica - ENE

Universidade de Brasília - UnB

Brasília, DF, Brasil

**Abstract.** *This work describes the design of a low cost 3D localization system based on strapdown IMU (Inertial Measurement Unit), GPS (Global Positioning System) and 3-axis magnetometer. Although part of an aerial robotics project, the applications of such systems range from virtual reality systems to sports training. The prototype has been built within the university facilities with low cost devices, whose performances in standalone operation for the task proposed is prohibitive. Hence, the sensors have been selected to compose an integrated navigation system, in which the IMU, built with micromachined inertial sensors, provides high sampling rate, but unbounded errors in long term operation; the GPS receiver provides position and velocity estimates without drift in long term operation; and the 3-axis magnetometer supplies information to correct attitude estimate. To perform the sensor fusion algorithm, a Kalman Filter, a 32-bit ARM microcontroller was selected, so embedded design issues are likewise discussed in the paper. Also, the initial alignment procedure and the filter equations using quaternions are described. Experimental results of this approach, which demonstrate the system performance, are presented, as well as a discussion about future improvements and different filter configurations.*

**Keywords:** *Low-cost 3D localization systems, Multi-sensor data fusion, Aerial robotics*

## 1. INTRODUCTION

Accurate and reliable 3D localization data is critical for aerial robots, because those vehicles normally present high instability when compared to robots that navigate on the ground or on the water. However, the employment of systems used in aeronautics may be prohibitive, since in many aerial robots there are weight, size, power and cost restrictions, particularly small and short range systems. Hence, it is of great interest the development of systems capable of real-time position, velocity and attitude estimation based on low cost MEMS (Micro-Electro-Mechanical Systems) sensors. Naturally, the applications of such a system may also be applied to other areas, from virtual reality to sports training.

Although environment perception technologies may be used in aerial robotics projects ([Ollero and Merino 2004]), specially in some specific operations, such as autonomous landing, in this work the sensors were selected in order to improve the versatility of the system. High performance inertial systems are widely employed in aerospace and naval systems, but, as the motion rate is used to estimate the vehicle position, unbounded errors occur in long term operation, specially on low cost units, due to the numeric integration of error factors. For that reason, absolute sensors, such as the GPS, must be used to correct the estimation provided by the IMU.

Numerous works dealing with integration of low cost IMU and other sensors, particularly GPS receivers, have been published. In [Kingston and Beard 2004], separate Extended Kalman Filters (EKF) for attitude and position are used to integrate data from an IMU, GPS, airspeed sensor and altimeter. In [van der Merwe 2004] the use of an Unscented Kalman Filter (UKF) as the sensor fusion algorithm is described. National research has also been conducted about the topic. The integration of an IMU with an speed sensor is described in [Santana et al. 2004] and in [Hemerly and Schad 2004] the application of an EKF not only to integrate data from IMU and GPS, but also to perform online sensor bias calibration, is reported.

The literature regarding a system composed by an IMU, GPS and 3-axis magnetometer, however, is not abundant. In [Vasconcelos et al. 2004] the same set of sensors is used, but the integration is performed with suboptimal complementary filters and Euler angles, which are known to exhibit singularities, are used to represent the attitude. Often IMU and 3-axis magnetometer are used to address the problem of attitude determination alone. In [Metnia et al. 2006] this set of sensors to estimate attitude and the gyrometer bias is also used, while [Marins et al. 2001] proposes a quaternion-based EKF to integrate the data.

In this paper, the development of a 3D localization system based on IMU, GPS and 3-axis magnetometer is described. The system was designed and completely built within the university facilities. A 32-bit ARM microcontroller was chosen to perform the integration algorithm. The magnetometer is used to improve the attitude estimation, while the GPS receiver provides absolute position and velocity estimates in Earth coordinates. Both sensors have lower sampling frequencies, when compared to the analog inertial sensors employed. Differently from [Vasconcelos et al. 2004], an EKF is used to integrate the data from all the sensors and to provide estimation of attitude represented in quaternions and position and

Table 1. Conventions adopted.

Symbol	Convention
$\mathbf{p}^m$	$3 \times 1$ vector $\mathbf{p}$ expressed in the $m$ -frame.
$\mathbf{C}_f^m$	$3 \times 3$ Direction Cosine Matrix (DCM) that transforms vector from the $m$ -frame to the $f$ -frame.
$q_f^m$	$4 \times 1$ quaternion that transforms vector from the $m$ -frame to the $f$ -frame.
$\boldsymbol{\omega}_{fm}^m$	$3 \times 1$ vector representing angular rates from the $m$ -frame with respect to the $f$ -frame expressed in measurements in the $m$ -frame.

velocity expressed in the reference frame. Also, the filter designed may be employed not only to perform bias online calibration, like [Hemerly and Schad 2004, Metnia et al. 2006], but also to perform scale factor online calibration of the inertial sensors. Although this feature has not been experimentally evaluated in this paper, it is an interesting approach, considering that accurate and low cost calibration procedures for scale factor are not available. Results that compare the quality of the 3D localization estimates in different operation conditions are also presented.

The paper is organized as follows. The first two Sections briefly discuss the sensors employed in the system and the the fusion algorithm, the EKF. Then, the prototype is presented in Section 4. Experimental results and further discussions are presented in the following Section. Finally, concluding remarks are pointed out in the last Section.

## 2. SENSORS

This Section describes the low cost sensors used in the 3D localization system proposed. The Tab. 1 presents some of the conventions adopted throughout the text, while the Fig. 1 illustrates some of the reference coordinate frames. It important to remark that, in this work, the origin of the  $n$ -frame is hold still during the operation of the device, mainly due to its short operation time, which is a different approach when compared to the traditional  $n$ -frame definition ([Titterton and Weston 1997]). A detailed description about quaternions, extensively used in this paper, and its use to represent attitude may be found in [Kuipers 1998].

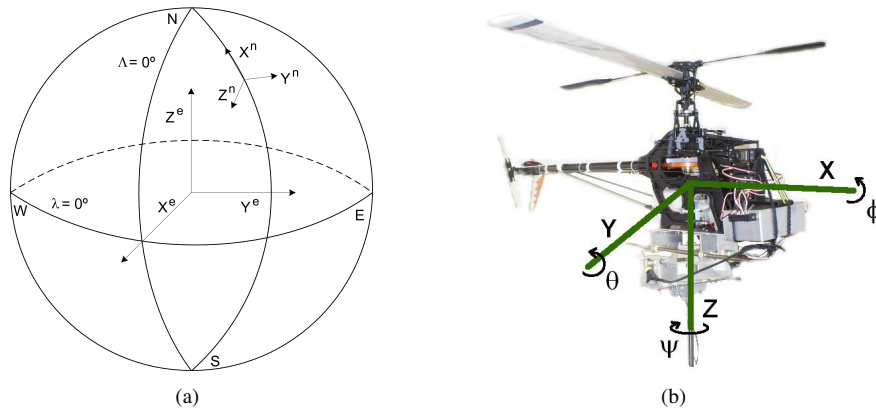


Figure 1. Coordinate frames definitions. (a) shows the Earth frame ( $e$ -frame) and the local geographic navigation frame ( $n$ -frame), while (b) illustrates the body frame ( $b$ -frame).  $\Lambda$  represents the longitude, while  $\lambda$  represents the latitude.

### 2.1 Inertial Measurement Unit

Inertial navigation is based on measuring the vehicle motion rate, as well as its initial position and attitude, to estimate its state throughout time. An Inertial Measurement Unit is normally composed by a 3-axis accelerometer, used to measure linear acceleration, and a 3-axis gyrometer, which measures angular rate. When those measurements are processed by a navigation algorithm in order to provide position, velocity and attitude estimates, the resulting system becomes an Inertial Navigation System (INS) [Titterton and Weston 1997].

In a strapdown IMU, the sensors are attached to the vehicle body, defining the body reference frame, or  $b$ -frame. The information provided by the gyrometers is used to transform the measurements in the  $b$ -frame to the chosen reference frame. Strapdown IMUs are opposed to gimbaled IMUs, in which the sensors are surrounded by gimbals in order to isolate the sensor set from rotations executed by the vehicle.

Usually, accelerometers are sensors that measure the force required to maintain a proof mass within the device case. As the proof mass is known, acceleration may be calculated. However, the sensor is not able to distinguish between acceleration caused by gravity from acceleration induced from other forces applied on the vehicle body, the inertial

acceleration. For that reason, it is considered that accelerometers actually measure the specific force,  $\mathbf{f}^b$ , with respect to an inertial frame.  $\mathbf{f}^b$  is given by

$$\mathbf{f}^b = \mathbf{a}^b - \mathbf{g}^b, \quad (1)$$

where  $\mathbf{a}$  and  $\mathbf{g}$  are the inertial and gravitational acceleration, respectively.

On the other hand, gyrometers measure angular rate with respect to an inertial frame. The gyrometers employed in the system proposed in this work actually measure the Coriolis acceleration caused on a proof mass by the rotation of the device. As the system operates on the Earth's surface, measurements from gyrometers and accelerometers, are affected by Earth's rotation,  $\omega_e \approx 15^\circ/\text{hour}$ . In this work, however, as the system operation time and the effects caused by Earth's rotation are modest when compared to sensor noise, those effects are neglected.

Under those considerations, attitude propagation from measurements of angular rates with respect to a known initial attitude is given by the following kinematic equation:

$$\begin{aligned} \dot{q}_n^b &= \frac{1}{2} \dot{q}_n^b \otimes \begin{bmatrix} 0 \\ \omega_{nb}^b \end{bmatrix} = -\frac{1}{2} \mathbf{W}_{nb}^b \dot{q}_n^b \\ &= -\frac{1}{2} \begin{bmatrix} 0 & \omega_x & \omega_y & \omega_z \\ -\omega_x & 0 & -\omega_z & \omega_y \\ -\omega_y & \omega_z & 0 & -\omega_x \\ -\omega_z & -\omega_y & \omega_x & 0 \end{bmatrix} \dot{q}_n^b, \end{aligned} \quad (2)$$

where  $\otimes$  defines a quaternion product.

Velocity and position expressed in the reference  $n$ -frame are given by

$$\dot{\mathbf{v}}^n = \mathbf{C}_n^b \mathbf{f}^b + \mathbf{g}^n \quad (3)$$

$$\dot{\mathbf{r}}^n = \mathbf{v}^n. \quad (4)$$

With high performance IMUs, the Eqs. (2) to (4) may provide satisfactory estimations of the vehicle position over long term operation. However, in an IMU built with low cost devices, the sensor errors, specially the bias, will probably cause the estimation to diverge within seconds. For that reason, absolute sensors, like the GPS receiver, must be used in a localization system that will be applied to aerial robots.

## 2.2 Global Positioning System

The Global Positioning System is a satellite-based radio localization system. The system is composed by 24 or more satellites, which send signals that can be interpreted by proper receivers. Once the distances from three or more satellites to the receiver are estimated, its position may be calculated. The problem of calculating an object position from its distance to three or more known reference points is called trilateration. Velocity estimates may also be calculated based on the Doppler effect, and for that they can be considered quite decorrelated from position information.

Nonetheless, GPS estimates may be corrupted by several time-correlated error sources. The major error source, the desynchronization of the receiver and the satellite clock, may be estimated when more than three satellites are available. Other source errors, however, are difficult to be directly estimated, like atmospheric effects or signal reflection due to surrounding obstacles. For real-time applications, an additional problem of GPS data is the low sampling frequency. Modern receivers usually do not provide position and velocity in rates higher than 4 Hz. The receiver used in this work has a maximum sampling frequency of 1 Hz.

In the literature of INS/GPS integration ([Grewal, Weill and Andrews 2001]), the sensor fusion algorithms may be classified as tightly or loosely coupled. Tightly coupled filters apply raw measurements from the GPS receiver, while loosely coupled filters apply preprocessed position and velocity data. In this work, the proposed architecture may be classified as loosely coupled. However, as the receiver position is expressed in the  $e$ -frame, since the satellites positions are also expressed in the  $e$ -frame, those estimates must be transformed to the  $n$ -frame. The DCM that transforms vectors in  $e$ -frame to the  $n$ -frame is given by

$$\mathbf{C}_n^e = \begin{bmatrix} -\sin \lambda \cos \Lambda & -\sin \lambda \sin \Lambda & \cos \lambda \\ -\sin \Lambda & \cos \Lambda & 0 \\ -\cos \lambda \cos \Lambda & -\cos \lambda \sin \Lambda & -\sin \lambda \end{bmatrix}, \quad (5)$$

where  $\Lambda$  and  $\lambda$  may be calculated from equations presented in [Tsui 2005].

From the estimated matrix  $\hat{\mathbf{C}}_n^e$ , consecutive positions estimates provided by the GPS receiver may be expressed in the  $n$ -frame with the following equation:

$$\mathbf{r}_{gps}^n(k) = \hat{\mathbf{C}}_n^e (\mathbf{r}_{gps}^e(k) - \hat{\mathbf{r}}^e(0)), \quad (6)$$

where  $\hat{\mathbf{C}}_n^e$  and  $\hat{\mathbf{r}}^e(0)$ , which is the estimated origin of the  $n$ -frame, are calculated from data provided by the GPS, as described in Section 3.



In addition to the observations provided by the GPS and by the 3-axis magnetometer and accelerometer, another measurement is considered. It is a pseudo-observation of the error on the quaternion norm,  $\|q_n^b\|$ . This pseudo-observation is applied because quaternions, when representing attitude, must have unity norm. Errors occur in the quaternion norm due to numeric integration and the filter corrections applied to the quaternion states. In order to minimize this problem, the following pseudo-observation is assumed:

$$e = 1 - \|q_n^b\|. \quad (9)$$

The correction by the pseudo-observation, which may also accomplish an additive noise, so the speed of convergence to the unity-norm quaternion may be tuned, can be applied after each prediction step. When measurements from the absolute sensors are available, those observations are included in the correction step. If all correction sources are available at the same instant, the following observation vector is applied:

$$\mathbf{y}(k+1) = \begin{bmatrix} q_n^b(k+1) \\ \mathbf{v}^n(k+1) \\ \mathbf{r}^n(k+1) \\ 1 - \|q_n^b(k+1)\| \end{bmatrix}. \quad (10)$$

The process and measurement noise were regarded as time-invariant additive white noise and the covariance matrices  $\mathbf{Q}$  and  $\mathbf{R}$  were selected experimentally. Future works will attempt to directly propagate both the IMU and the TRIAD algorithm covariances from sensor noises and develop an accurate error model for the GPS outputs.

### 3.1 System initialization

The integration filter described is able to estimate the 3D localization throughout time from the present state and the measurements obtained from the sensors. Hence, a good estimate of the initial state must be provided, so that the filter may achieve high performance.

The selection of initial position and velocity states are not critical, since, at least in some applications, the system may be hold still in the initialization period. In this case, GPS position information from the initialization period may be used to calculate  $\mathbf{C}_n^e$  and  $\mathbf{r}^e(0)$ , which define the reference  $n$ -frame used in this work. Hence, the initial position and velocity states could be simply considered zero.

On the other hand, the choice of an accurate attitude initial state, a procedure known as initial alignment, is crucial for the performance of the 3D localization system, specially when such a system is applied to aerial robots. From Eq. (8), it is clear that errors on  $q_n^b$  will lead to great errors on  $\mathbf{r}^n$ , since the specific force  $\mathbf{f}^b$  measured by the accelerometer contains the gravity component (Eq. (1)). Moreover, in aerial robotics, an accurate estimate of the vehicle attitude is essential for the vehicle stability and navigation, since its control system lowest level is the attitude controller.

In the proposed system, the attitude initial state is computed from  $\mathbf{m}^b$  and  $\mathbf{f}^b$ , which are measured by the magnetometer and accelerometer, respectively. The Improved TRIAD algorithm may be directly employed, as  $\mathbf{g}^n = [0 \ 0 \ g]^T$  and  $\mathbf{m}^n$  may be obtained from maps of the Earth's magnetic field. As both sensors have been previously calibrated and the vehicle is still during the initialization period,  $\mathbf{f}^b$  provides a good estimate of  $\mathbf{g}^b$ .  $\mathbf{m}^b$ , instead, may be corrupted by the presence of other magnetic fields and ferrous materials, which can degenerate the initial attitude state.

### 3.2 Online sensor calibration

The low cost inertial sensors used in this work present an error model with bias, scale factor error, time-varying parameters, such as turn on-to-turn on bias, misalignment errors and others. Furthermore, due to the low cost nature of the project, the cost of calibration techniques that require other equipments, as described in [Titterton and Weston 1997], are prohibitive. Therefore, online calibration procedures, as proposed for instance by [Hemerly and Schad 2004], are of great interest.

In this paper, the following error model is assumed for the inertial sensors, illustrated by the accelerometer measurement along the  $X$  axis:

$$\tilde{f}_x^b = s_{f_x} f_x^b + b_{f_x} + w_{f_x}, \quad (11)$$

where  $\tilde{f}_x^b$  is the measurement corrupted by errors provided by the accelerometer,  $f_x^b$  is the true value of the specific force along the  $X$  axis and  $b_{f_x}$ ,  $s_{f_x}$  and  $w_{f_x}$  are the bias, the scale factor and the associated noise, respectively.

Based on the model represented by Eq. (11), the sensor error parameters are included in the integration as states to be estimated. Bias and scale factor evolves in accordance with

$$\mathbf{b}(k+1) = \mathbf{b}(k) + \mathbf{w}_b \quad (12)$$

$$\mathbf{s}(k+1) = \mathbf{s}(k) + \mathbf{w}_s. \quad (13)$$

Table 2. Components specifications. Source: Sparkfun Electronics and Digikey Corporation.

Device	Model (Manufacturer)	Unity price [US\$]
Gyrometer $Z$	ADXRS150 (Analog Devices)	36,00
Gyrometer $X$ e $Y$	IDG300 (Invensense)	54,00
3-axis Accelerometer	MMA7260QT (Freescale)	9,00
3-axis Magnetometer	MicroMag3 (PNI)	60,00
GPS receiver	ET-102 (Globalsat)	60,00

Thus, in this new configuration, the filter state vector presents 22 states. The initial states for the sensor parameters are given by prior calibration, in the case of accelerometers, or calculated during the initialization procedure, in the case of gyrometers bias. The initial covariance matrix  $\mathbf{P}$  associated with those states have low magnitude, so that the speed of convergence is held slow.

#### 4. SYSTEM DESIGN

This Section describes the prototype design and assembled in order to evaluate the algorithms presented in the previous Sections with low cost sensors. The decision to build the prototype within the university facilities has prevented higher miniaturization of the system, represented on Fig. 3(a).

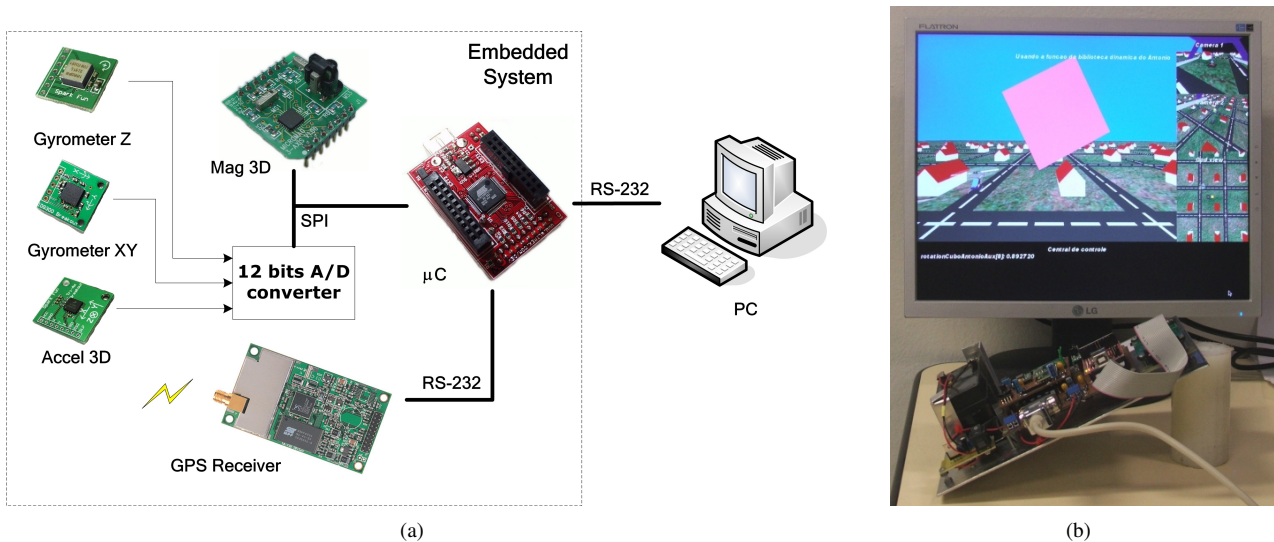


Figure 3. The 3D localization built within the university facilities.

During system design, great effort has been made to guarantee an orthogonal configuration of the sensors measurement axes. Likewise, in order to avoid interference caused by positioning the analog sensors near high frequency digital tracks and increase the system modularity, the prototype was built with two separate printed circuit boards. Furthermore, it is also worth mentioning that, unlike many low cost IMU designs, the prototype developed has all inertial sensors standing on the same plane, since that two types of gyrometers were used: a sensor sensitive to rotations about the  $Z$  axis and another IC with two sensors integrated, which are sensitive to rotations about the remaining axes. Table 2 presents the components used in the prototype, as well as respective unity prices, excluding import taxes and delivery costs.

The sensor fusion algorithm is implemented in a AT91SAM7S64 microcontroller, from Atmel, which is based on a 32-bit AMR7 core. With this microcontroller, the filter is able to execute in a sampling frequency of  $50\text{ Hz}$ . Data is transmitted to a PC through a RS-232 interface. Figure 3(b) shows real-time evaluation of the attitude estimated by the EKF. The estimate computed by the prototype is sent to the PC, in which the result can be evaluated in a 3D simulation environment.

#### 5. EXPERIMENTAL RESULTS

In order to evaluate the performance of the proposed system, outdoor experiments were conducted at the university campus. The 3D localization system was installed in a car and a PC operated as a data-logger. The 40-second initialization period was executed as described in Sec. 3 and the test, which was conducted under normal traffic conditions, lasted about 220 seconds. The results obtained are shown in Fig. 4. It is important to mention that, although the system operated

strapped to a car, hence with limited motion over the  $Z^n$  axis, no restrictions were imposed to the EKF.

Based on the results, it can be stated that the system presented good performance. From the test initial position, the origin of the  $n$ -frame, the vehicle was conducted toward North. It can be seen that the system presented robustness against cases where a single GPS measurement was lost. The quality of the estimates provided by the EKF were decreased only when the GPS solution was unavailable for a long period. Figure 4 indicates with three succeeding arrows the case in which there was a 4-second GPS gap, a moment when the system estimates were unsatisfactory.

Other experiments were conducted under different conditions. When the magnetometer operated under the effect of another magnetic field, for instance, the system presented robustness against that effect, although the attitude estimation was not as good as the performance presented in Fig. 4. On the other hand, when the magnetometer and the pseudo-observation were not used, the attitude estimate was unsatisfactory, specially when large corrections were applied by the filter due to the arrival of GPS measurements after a period of absence.

It also can be seen in Fig. 4 that the path followed by the car was not around an open area, as there are buildings and trees nearby. Considering those conditions, the GPS performance was satisfactory. Still, following prototypes will use more advanced GPS receivers, which may also provide raw information to the user, so that a tightly coupled integration filter may be implemented.

## 6. CONCLUSIONS

In this work, the development and experimental evaluation of a 3D localization system based on low cost sensors for application on aerial robots was presented. The system integrates data from an IMU, a GPS receiver and a 3-axis magnetometer to provide position and velocity expressed in the reference frame and attitude represented in quaternions. An EKF was used as the sensor fusion algorithm. Results show that the approach provides good performance and that the attitude estimate is improved with the use of a magnetometer. Moreover, it is shown that the performance is acceptable even when poor conditions, like GPS loss for short periods, are present.

## 7. ACKNOWLEDGEMENTS

The authors would like to thank the other members of the CARCARAH Project for their support, specially Alexandre Simões Martins, for the assistance during outdoor experiments, and Bruno Vilhena Adorno, who developed the simulator used for attitude real-time testing. Also, it is important to mention the contribution of the Dynamic Metrology Laboratory from the University of Brasília for the value of the local gravitational field,  $g$ .

## 8. REFERENCES

- GREWAL, M. S.; WEILL, L. R.; ANDREWS, A. P. *Global Positioning Systems, Inertial Navigation and Integration*. [S.l.]: John Wiley & Sons, 2001.
- HEMERLY, E. M.; SCHAD, V. R. Sistema de navegação de baixo custo baseado na fusão INS/GPS usando filtro de kalman. In: *XV Congresso Brasileiro de Automática*. [S.l.: s.n.], 2004.
- KINGSTON, D.; BEARD, R. Real-time attitude and position estimation for small UAVs using low-cost sensors. In: *AIAA 3rd Unmanned Unlimited Technical Conference, Workshop and Exhibit*. [S.l.: s.n.], 2004.
- KUIPERS, J. B. *Quaternions and rotation sequences: a primer with applications to orbits, aerospace, and virtual reality*. [S.l.]: Princeton University Press, 1998.
- LI, Y.; YUAN, J. Attitude determination using GPS vector observations. *GNSS World of China*, v. 33, n. 3, p. 51–56, 2005.
- MARINS, J. L. et al. An extended Kalman filter for quaternion-based orientation estimation using MARG sensors. In: *IEEE International Conference on Intelligent Robots and Systems*. [S.l.: s.n.], 2001.
- METNIA, N. et al. Attitude and gyro bias estimation for a VTOL UAV. *Control Engineering Practice*, v. 14, n. 12, p. 1511–1520, 2006.
- OLLERO, A.; MERINO, L. Control and perception techniques for aerial robotics. *Annual Reviews in Control*, v. 28, p. 167–178, 2004.
- ROGERS, R. M. *Applied mathematics in integrated navigation systems*. [S.l.]: AIAA Education Series, 2003.
- SANTANA, D. S. et al. Estimação de trajetórias utilizando sistema de navegação inercial strapdown. In: *XV Congresso Brasileiro de Automática*. [S.l.: s.n.], 2004.
- TITTERTON, D. H.; WESTON, J. L. *Strapdown inertial navigation technology*. [S.l.]: Peter Peregrinus LTD. on behalf of the Institution of Electrical Engineers, 1997.
- TSUI, J. B.-Y. *Fundamentals of Global Positioning Systems Receivers: a Software Approach*. [S.l.]: John Wiley & Sons, 2005.
- van der Merwe, R. *Sigma-Point Kalman Filters for Probabilistic Inference in Dynamic State-Space Models*. Tese (Doutorado) — Oregon Health & Science University, USA, 2004.
- VASCONCELOS, J. et al. GPS aided IMU for unmanned air vehicles. In: *5th IFAC/EURON Symposium on Intelligent Autonomous Vehicles*. [S.l.: s.n.], 2004.

## 9. Responsibility notice

The authors are the only responsible for the printed material included in this paper

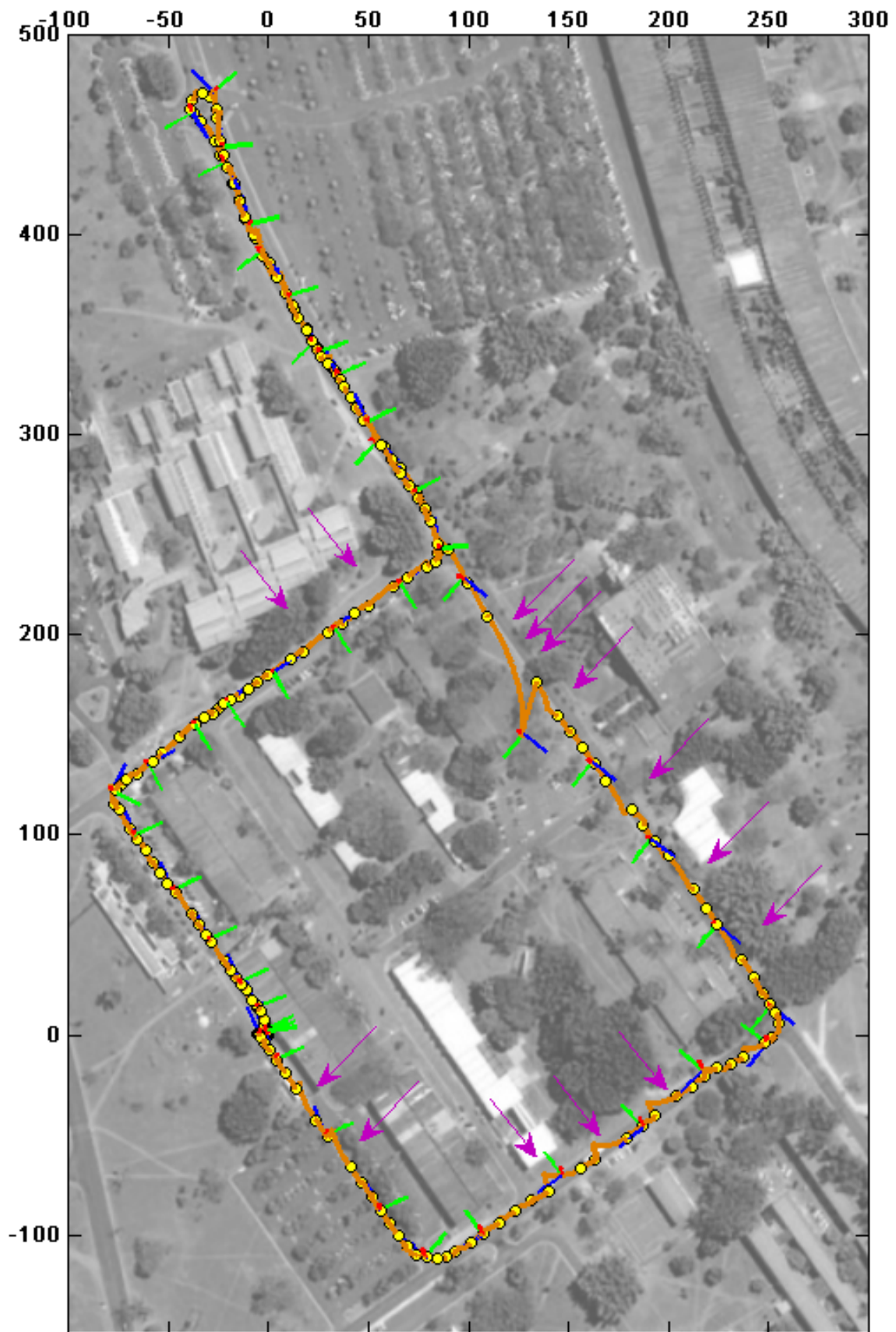


Figure 4. System performance when all the available sensors were integrated. The estimated position is shown in orange, the attitude in a RGB frame and the GPS positions are represented by yellow dots. The purple arrows point to locations where the GPS receiver did not reach a valid solution. Y axis represents the North direction, while the X axis represents points to the East. Source: Google Earth.